A Digital Acoustic Recording Tag for Measuring the Response of Wild Marine Mammals to Sound

Mark P. Johnson and Peter L. Tyack

***Abstract*—Definitive studies on the response of marine mammals to anthropogenic sound are hampered by the short surface time and deep-diving lifestyle of many species. A novel archival tag, called the DTAG, has been developed to monitor the behavior of marine mammals, and their response to sound, continuously throughout the dive cycle. The tag contains a large array of solid-state memory and records continuously from a built-in hydrophone and suite of sensors. The sensors sample the orientation of the animal in three dimensions with sufficient speed and resolution to capture individual fluke strokes. Audio and sensor recording is synchronous so the relative timing of sounds and motion can be determined precisely. The DTAG has been attached to more than 30 northern right whales (*Eubalaena glacialis*) and 20 sperm whales (*Physeter macrocephalus*) with recording duration of up to 12 h per deployment. Several deployments have included sound playbacks to the tagged whale and a transient response to at least one playback is evident in the tag data.**

***Index Terms*—Effects of noise, marine animals, tags, underwater acoustic measurements.**

I. Introduction

VER THE PAST century, economic and technological developments have increased the human contribution to ambient noise in the ocean. Although shipping is the overwhelmingly dominant source of manmade noise in the ocean [1], a wide variety of artificial sound sources also contribute to the ambient sound field, examples being air guns, used in seismic exploration, sonar, and acoustic navigation, and telemetry sources. There is growing evidence that man-made sounds can disturb marine mammals, and this issue has received increasing attention [2], [3]. Observed responses include silencing, disruption of activity, lengthening of song, movement away from the source, and perhaps even stranding [3, ch. 9]–[5]. The zone of influence of a sound source depends upon its level, its frequency spectrum, its significance to the animal, and upon the conditions for sound propagation near the source [3, ch. 10]. Sound carries so well underwater that animals may be affected many tens of kilometers away from a loud source [6], [7], and there is no *a priori* reason to rule out effects at even greater ranges. Marine mammals rely on sound for communication, orientation, and detection of predators and prey; disruption of any of these functions would interfere with normal activities and behavior. This raises the concern that, along with short-term impacts of single sources, increasing noise may have long-term impact as a form of habitat degradation.

Research on the effects of noise on large whales has suffered from a lack of methods to observe behavior in sufficient detail. Many deep diving species are visible only 5% of the time, when they are breathing at the surface, so visual observations are seldom adequate. Passive acoustic monitoring of whales is often hindered by a lack of knowledge of the species repertoire and whether a change in vocal output can be expected in response to noise. Moreover, in animals that are thought to silence in response to noise (e.g., sperm whales [8]), passive acoustic tracking may be impossible following an exposure, making it difficult to assess the magnitude of response.

Acoustic recording tags represent a new technological solution for monitoring disturbance reactions of marine mammals. The concept here is to measure the sound environment of the animal in tandem with physiological or behavioral information. By comparing the timing of any change in behavior to the sound as heard by the animal, causality can be established in controlled experimental exposures of sound. The extent of the response can then be gauged against received sound level, the first step toward determining suitable exposure limits for a given sound. Early examples of acoustic recording tags are those of Burgess *et al.* [9], developed for deep-diving elephant seals, and Fletcher *et al.* [10], who used such a tag to study the effects of an ATOC transmitter on the dive patterns of seals. Behavioral and physiological sensing on both of these tags was limited to depth of dive although Burgess found a heartbeat sound in the audio record from elephant seals [9]. In an effort to extend behavioral sensing, Tyack, Johnson, and Nowacek combined a miniature digital audio tape (DAT) recorder with an orientation sensor in 1998 [11]. Various versions of this tag were deployed on wild bottlenose dolphin and northern right whales, proving the feasibility of on-animal sound and orientation measurement.

An effort funded by the Office of Naval Research (ONR) to reduce the size and increase the capabilities of acoustic recording tags resulted in the development of the DTAG in 1999. This tag uses FLASH memory in place of moving magnetic tape or disks to record data and so can be encapsulated in plastic. A low-power digital signal processor combines audio, acquired from a hydrophone, with sensor measurements, and streams the data to the nonvolatile memory array. The sensor suite comprises acceleration, magnetic field, and pressure sensors and is tailored to measuring orientation at sampling rates of up to 50 Hz, much higher than traditional time–depth recorders.

Manuscript received May 2001; revised August 2002. This work was supported in part by the Office of Naval Research under Grants N00014-99-10831 and N00014-99-10819, in part by the National Marine Fisheries Service (NMFS) under Grant NA87RJ0445, in part by the Strategic Environment Research Development Program (SERDP) under Grant CS-1188, in part by the International Fund for Animal Welfare, and in part by the Ida and Cecil Green Technology Development Award.

The authors are with the Woods Hole Oceanographic Institution, Woods Hole, MA 02543 USA.

Digital Object Identifier 10.1109/JOE.2002.808212

In this paper, the design of the new tag is presented together with results demonstrating its potential for studying the response of marine mammals to acoustic stimuli. The following section describes the tag and the means by which it is attached to wild marine mammals. Section III deals with estimation of orientation from the DTAG sensors. Although orientation measurement is a well-established technique, being the mainstay of navigation systems in underwater vehicles and aircraft, its application to marine mammals is new. Section III focuses on the issues that arise in estimating the orientation of marine mammals with sub-fluke-stroke time resolution and the supporting visual observations needed to determine movement in a global frame. Some quality metrics implicit in the measurement are also highlighted. The remainder of the paper is devoted to a series of examples taken from tag deployments on northern right whales and sperm whales. Two possible responses to controlled sound playbacks are examined to demonstrate the power of the new tag in parameterizing responses, and the confounds implicit in such fine-scale analyses.

II. DTAG Design

The governing constraints on the DTAG design are that it be small, lightweight, pressure tolerant and have a substantial recording time. Although the large whales of primary interest here can carry a big tag, the problems involved in delivering and attaching the tag to the animal, scale strongly with tag size and weight. Options for tag delivery include a long pole, gun, or crossbow, all of which require a small, light payload. The tag must also be tolerant to the pressure experienced during deep dives. Evidence exists for sperm whale dives in excess of 2000 m [12] corresponding to a hydrostatic pressure of over 20 MPa.

The recording time of the tag is determined by its memory capacity and audio sampling rate. For the typical controlled sound experiment, a recording time of at least 4 h is needed. This allows at least two dives after tag delivery to establish a behavioral baseline for the animal, even for animals with hour-long dives, followed by a sound playback of 1 h and a 1-h post-exposure period. Based on the frequency range of their vocalizations, suitable sampling rates for baleen and sperm whales are in the 10–50-kHz range. A minimum memory capacity of 200–1000 MB is thus required (e.g., 12 b per sample $\times$ 16 kHz $\times$ 4 h $=$ 350 MB). More memory is desirable as then a longer interval can be left between tagging and sound playback, increasing the chance of observing a natural response. A long recording time after an exposure is also desirable to better observe the return to baseline behavior.

A tag design meeting the above constraints is illustrated in the block diagram of Fig. 1 along with a photograph of the complete electronics package. The design centers on a low-power programmable digital signal processor (DSP) which combines data from the audio and sensor circuits and stores the result to a memory array. Although the sampling-rates of the audio and sensor signals necessarily differ, synchrony is maintained by acquiring a precise number of audio samples between each sensor sample. Use of a DSP also enables real-time filtering and compression of the signal streams when required. When the tag is not recording, the DSP performs the user interface and data-offloading functions. An infrared interface with a data rate of 0.5 MB/s is used to program the tag and to recover data. As initially designed, the DTAG had 400 MB of FLASH memory but increases in component density now allow up to 3 GB in the same size tag.

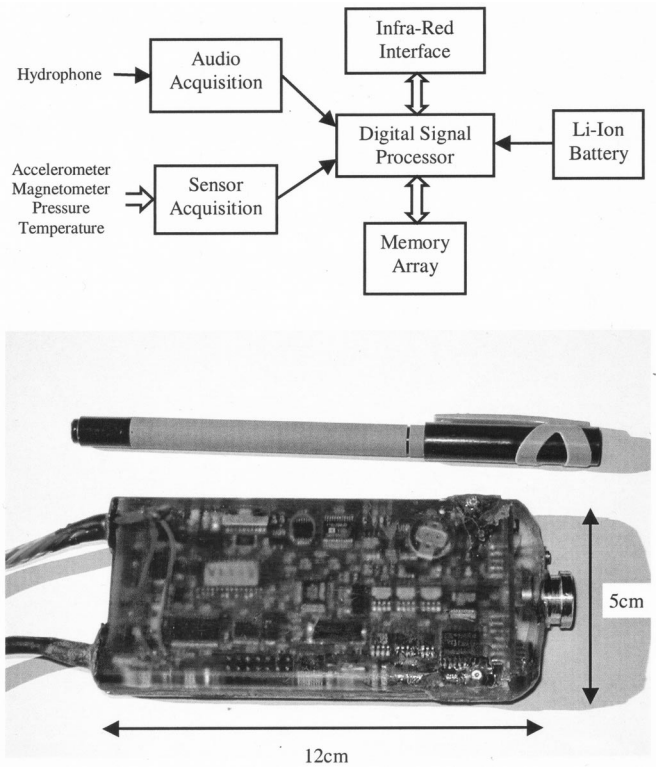

Fig. 1. Simplified block diagram of the DTAG (above) and photograph of the encapsulated electronics package (below). The leads on the left of the tag are for battery and hydrophone.

The audio subsystem in the tag consists of a piezo-ceramic hydrophone, a preamplifier, anti-alias filter and analog-to-digital converter (ADC). A 12-b ADC is used with sampling-rate programmable between 2–200 kHz. The anti-alias filter cut-off frequency and preamplifier gain are also programmable. With gain set to 12 dB, the dynamic range of the tag audio recording is from 80 dB (noise floor) to 152 dB (onset of clipping) re 1 μPa. With this gain, good fidelity recording of distant animals and vessels is obtained at the expense of clipping during loud vocalizations from the tagged whale.

The tag has sensors for depth, temperature, and orientation. Depth is determined from a pressure sensor with a resolution of 0.5 m$\cdot H_2O$ over a range of 0–2000 m. Orientation, parameterized by the Euler angles: pitch, roll, and heading, requires two sets of sensors. Pitch and roll are measured by capacitive accelerometers (Analog Devices ADXL202). These sense both the dynamic acceleration of the tagged whale and its orientation with respect to the gravity vector. The spatial freedom enjoyed by a submerged animal necessitate a 360° measurement range for pitch and roll requiring, in turn, a three-axis accelerometer. The heading sensor uses a three-axis magnetometer to measure the direction of the earth's magnetic field relative to the tag. Each magnetometer axis comprises a low-power magnetoresistive bridge sensor (Honeywell HMC1021). To estimate heading,

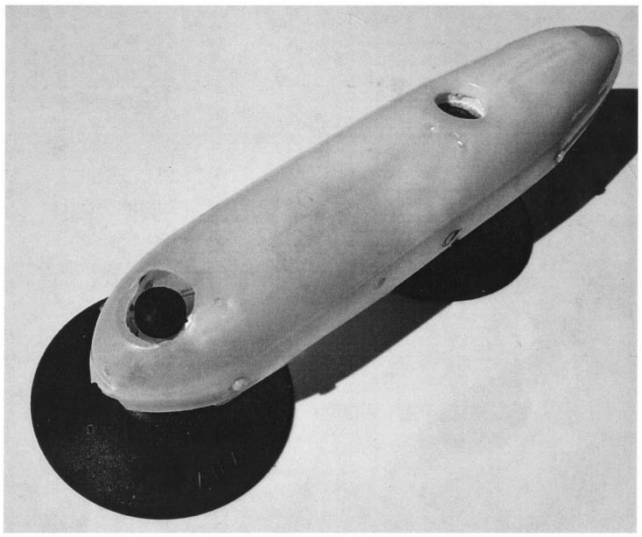

Fig. 2. Complete tag including plastic fairing, floatation, and two suction cups (front of tag is to the left).

the three magnetometer signals are corrected for pitch and roll. This process, called gimballing in analogy to the floating needles used in traditional compasses, effectively transforms the magnetic-field measurement to that which would be made on a horizontal surface with the same heading. The method of orientation estimation is the subject of Section III.

To avoid a heavy pressure housing, the DTAG circuit boards are encapsulated in epoxy resin. This provides electrical isolation but does not fully insulate the circuitry from hydrostatic pressure. It is thus crucial to select components that are robust to high pressure and to eliminate air bubbles during potting. A low-viscosity resin was selected for this reason. The complete encapsulated DTAG has been tested to a water depth of 2000 m and functioned satisfactorily. Although the components in the tag are pressure tolerant, their performance may vary with pressure. For example, the accelerometers have an output offset of about 0.002 $m{\cdot}s^{-2}$ per meter of water depth. The power consumption of the DTAG is about 150 mW while recording and this can be met with a single 3-Wh lithium polymer rechargeable cell. Polymer cells have a solid electrolyte and so are inherently pressure tolerant. To verify this, we have discharged polymer cells under pressure (2000 m H_2O) and have found no deviation from the discharge characteristic at atmospheric pressure.

Due to the short recording time of the DTAG, being designed for daily playback experiments, and the desire to minimally disturb the tagged animal, a noninvasive suction-cup attachment has been developed. Suction cups have been used widely with marine mammals [13] and attachment durations of tens of hours have been reported. For the DTAG to track orientation accurately, a rigid connection is required between the whale and the tag using at least two suction cups as shown in Fig. 2. A near-vertical force on the tag is needed to attach it to a whale and a system devised by Moore [14] for ultrasound inspection of right whale back fat has been adapted to deliver the DTAG. The system consists of a 12-m carbon-fiber pole, cantilevered in a bow-mounted oarlock, as shown in Fig. 3. The mounting provides four degrees of freedom: the pole may be rotated and

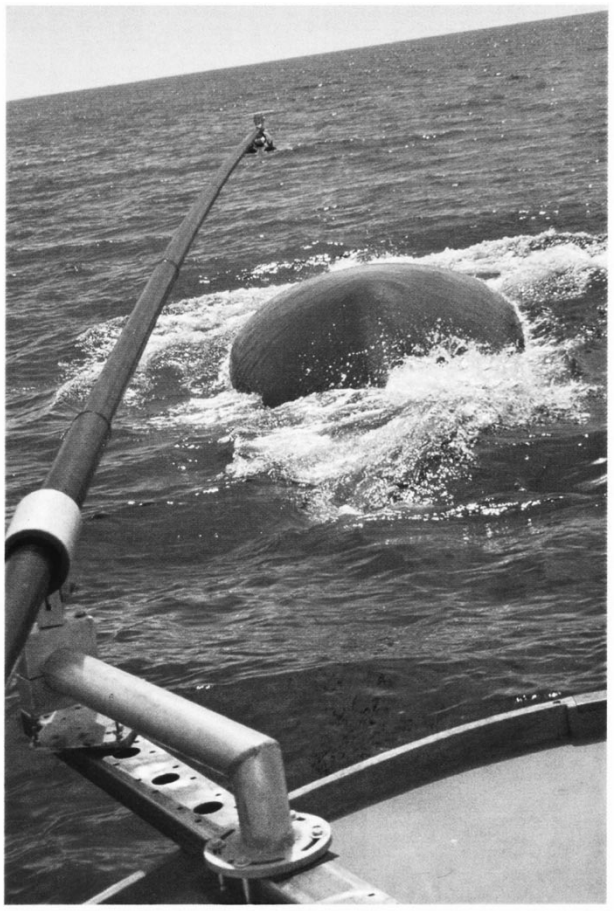

Fig. 3. Delivery of the tag to a northern right whale using a 12-m cantilevered pole developed by Moore [14].

can slide through the oarlock, and the oarlock itself swivels and tilts. The key advantage of the long pole is that it is possible to deliver the tag without encroaching over the flukes of the animal. As suction cups often release from an animal in a matter of hours due to leakage, our attachment includes a pump powered by the pressure changes during the whales' dive cycle to maintain vacuum in the cups. An active release is also included consisting of a nickel–chromium wire which seals a valve in the air line to each suction cup. The wire corrodes rapidly in seawater when made anodic and is controlled by a clock circuit in the DTAG.

The tag electronics, battery, very high frequency (VHF) radio beacon, and suction cups are housed in a thermoformed polyethylene hull to minimize drag. The hull is flooded to allow water to reach the pressure and temperature sensors. The rear section of the hull is filled with syntactic foam sufficient to float the tag tail-up when not attached, keeping the VHF antenna above the sea surface. The volume of the tag is about 1 liter and the dry weight is 500 g, making it acceptable for pole delivery.

Two versions of the DTAG, the two-cup design shown in Fig. 2 and a three-cup version, have been attached to over 30 northern right whales during three years of field work in the Bay of Fundy, Canada. The longest attachment time was 21 h and 33% of attachments lasted sufficiently long for a playback experiment (4 h). The DTAG has also been attached to about

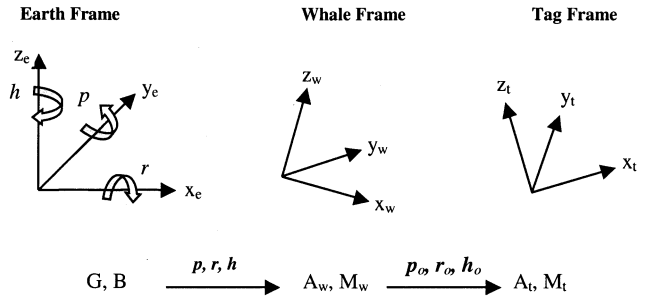

Fig. 4. Three frames of reference involved in determining whale orientation showing the rotational transformations between frames. In the earth frame, x is northward, y is westward, and z is upward. In the whale frame, x is rostrally directed and is the long axis of the animal. In the tag frame, x is the long axis of the tag pointing noseward.

20 sperm whales over three years in the Mediterranean Sea and the Gulf of Mexico. The longest attachment on sperm whales was 10 h, and 41% of attachments lasted longer than 4 h. A majority of early releases on right whales and some releases on sperm whales resulted from social interactions between animals in which the tag was rubbed off. Breaching of the tagged whale was another less frequent cause of early release. Rubbing and breaching are behaviors which few nonimplanted tags could be expected to survive and, in fact, may also lead to failure of implanted tags. We view movement or release of the suction cup tag, when stressed, not as a problem but a feature which reduces the chance of discomfort or minor injury to the tagged whale.

III. Orientation Estimation

A key innovation of the DTAG is its ability to measure the orientation of the tagged animal as a function of time. Orientation is deduced from the three-axis accelerometer and magnetometer signals and is expressed in terms of the Euler angles, pitch, roll, and heading, with reference to the fixed (earth) frame [15]. As the tag may be placed anywhere on the back of a whale, the tag axes do not generally coincide with the whale axes. There are thus three frames involved: the earth frame, the tag frame, and the whale frame, and these are related as shown in Fig. 4. Note that the definitions of heading and pitch in Fig. 4 differ from their standard Euler definitions: we have chosen heading to follow the compass convention and pitch is positive for a nose-upward tilt. Also, heading refers to magnetic heading and requires compensation for declination angle to obtain the true heading. The goal is to determine the orientation of the whale, i.e., the angles of rotation, p, r, and h, relating the whale frame to the earth frame. This is achieved in two steps. First the tag measurements are corrected for the orientation of the tag on the whale; then the whale frame angles, p, r, and h, are deduced from the corrected tag data.

If the whale is moving at a constant velocity, and measurement noise and sensor miscalibration are ignored, the three-axis acceleration and magnetic-field measurements made by the tag can be expressed as

$$\begin{aligned} A_t &= \mathbf{R}(r_o)\mathbf{P}(p_o)\mathbf{H}(h_o)\mathbf{R}(r)\mathbf{P}(p)\mathbf{H}(h)G \\ M_t &= \mathbf{R}(r_o)\mathbf{P}(p_o)\mathbf{H}(h_o)\mathbf{R}(r)\mathbf{P}(p)\mathbf{H}(h)B \end{aligned} \tag{1}$$

where $A_t = [a_{t,x}, a_{t,y}, a_{t,z}]^T$, and $M_t = [m_{t,x}, m_{t,y}, m_{t,z}]^T$, are the sensor outputs and the subscript t indicates the tag frame. $G = [0, 0, -g]^T$ is the gravity vector in the earth frame and g is the acceleration due to gravity. $B = b.[\cos(i), 0, -\sin(i)]^T$ is the magnetic-field vector in the earth frame, where b and i are the magnetic-field intensity and inclination angle, respectively. The rotation matrices in (1) are defined as

$$\mathbf{R}(\cdot) = \begin{bmatrix} 1 & 0 & 0 \\ 0 & \cos(\cdot) & \sin(\cdot) \\ 0 & -\sin(\cdot) & \cos(\cdot) \end{bmatrix}$$

$$\mathbf{P}(\cdot) = \begin{bmatrix} \cos(\cdot) & 0 & \sin(\cdot) \\ 0 & 1 & 0 \\ -\sin(\cdot) & 0 & \cos(\cdot) \end{bmatrix}$$

and

$$\mathbf{H}(\cdot) = \begin{bmatrix} \cos(\cdot) & \sin(\cdot) & 0 \\ -\sin(\cdot) & \cos(\cdot) & 0 \\ 0 & 0 & 1 \end{bmatrix}.$$

These matrices are not symmetric so the multiplication order in (1) is important.

The tag orientation on the whale is parameterized in (1) by the pitch, roll, and heading, p_o, r_o and h_o, of the tag with respect to the whale. Values for p_o, r_o, h_o (which may vary with time if the tag slides on the whale), can be measured from photographs of the tag but can also be deduced readily from visual and tag data. The location of the nares in most whale species necessitate a pitch and roll close to 0 when surfacing for breath. If the heading of the whale during surfacing is recorded by visual observers, a sequence of known whale orientations result which can be compared to the tag data to determine p_o, r_o and h_o. Once the tag orientation has been established, A_t and M_t can be converted to their whale-frame equivalents, that is, the sensor signals that would be measured if the tag was perfectly aligned on the whale

$$\begin{aligned} A_w &= \mathbf{H}^T(h_o)\mathbf{P}^T(p_o)\mathbf{R}^T(r_o)A_t \\ M_w &= \mathbf{H}^T(h_o)\mathbf{P}^T(p_o)\mathbf{R}^T(r_o)M_t \end{aligned} \tag{2}$$

where $\mathbf{H}^{-1} = \mathbf{H}^T$ for a rotation matrix. Combining (1) and (2)

$$A_w = \begin{bmatrix} a_{w,x} \\ a_{w,y} \\ a_{w,z} \end{bmatrix} = -g.\begin{bmatrix} \sin(p) \\ \cos(p)\sin(r) \\ \cos(p)\cos(r) \end{bmatrix}. \tag{3}$$

The whale pitch and roll can be estimated from the whale frame signals by

$$r = \mathrm{a}\tan\left(\frac{a_{w,y}}{a_{w,z}}\right) \quad \text{and} \quad p = \mathrm{a}\sin\left(a_{w,x}\right). \tag{4}$$

Note that a four-quadrant arctangent is required in (4) to estimate roll over the (−180 °–180 °) range. For reasons to be discussed, pitch is constrained to (−90 °, 90 °). Having calculated p and r, the heading can be determined by premultiplying the second line of (2) by $\mathbf{P}^T(p)\mathbf{R}^T(r)$ to get

$$M_h \triangleq \mathbf{P}^T(p)\mathbf{R}^T(r)M_w = \mathrm{b}.\begin{bmatrix} \cos(i)\cos(h) \\ -\cos(i)\sin(h) \\ -\sin(i) \end{bmatrix} \tag{5}$$

where M_h is the magnetometer measurement that would be made on a horizontal (i.e., gimballed) surface with the same

heading as the whale. Heading can then be estimated by $h = \mathrm{atan}(m_{h,y}/m_{h,x})$, again using a four-quadrant arctangent to realize a ($-180\,^\circ$–$180\,^\circ$) range.

The pitch, roll, heading parameterization of orientation is not unique: any orientation can be described by two sets of p, r, and h, say $\{p_1,\ r_1,\ h_1\}$ and $\{p_2,\ r_2,\ h_2\}$, both of which produce the same A_w and M_w. These are related as $p_2 = 180 - p_1$, $r_2 = 180 + r_1$, and $h_2 = 180 + h_1$. The ambiguity is a physical one. There are always two combinations of pitch, roll, and heading which result in the same orientation. For example, if the animal is upside-down, it may have attained this attitude by rolling $180\,^\circ$, or by changing heading by $180\,^\circ$ and pitching $180\,^\circ$. The ambiguity can be resolved by constraining p to ($-90\,^\circ$, $90\,^\circ$) and accepting jumps in roll and heading if the animal does pitch beyond $90\,^\circ$. An additional ambiguity arises when the animal is at $\pm 90\,^\circ$ pitch: in both cases, $a_{w,y}$ and $a_{w,z}$ become 0 and the roll is indeterminate.

The above results are for the unrealistic case of perfect, noise-free sensors. In practice, a number of factors degrade the orientation estimate. These include variations in sensitivity and zero offset between sensor axes, sensitivity changes due to changing pressure or temperature, measurement noise, and acceleration of the animal. The most significant of these is acceleration, which may result from swimming, rapid maneuvering, or even from waves slapping the tag when the animal surfaces. For the large whales of primary interest here, acceleration of the tag due to body undulations during swimming is likely to be small, with peak magnitude of less than 0.1 g for a 15-m animal with a 6-s fluke rate [16]. However, startle responses or fast feeding movements may produce large transient accelerations. Although use of a low-pass filter on the acceleration signals will reduce such transients, substantial orientation errors are still possible. Fortunately, there are three implicit quality metrics that facilitate detection of distorted measurements and which can provide a sample-by-sample estimate of orientation accuracy. First, the two-norm of the accelerometer vector, $v_a = (A_t^T A_t)^{1/2}$, should, in the absence of acceleration, miscalibration, and measurement noise, equal g. Likewise, the two-norm of M_t: $v_m = (M_t^T M_t)^{1/2}$, should equal b, the magnetic-field intensity. Finally, referring to (1) and recalling that rotation matrices are unitary, the dot-product of A_t and M_t should equal $G.B = v_a v_m \sin i$, i.e., the product of g, b, and the sine of the magnetic-field inclination angle. Although b and i vary geographically, they do so gradually and will be essentially constant over a deployment area. Therefore, any deviation of v_a, v_m, or $A_t.M_t$, from their nominal values sheds doubt on the accuracy of the orientation estimate. Epochs of high acceleration and so high orientation error can be identified readily by examining the time series of v_a, v_m, and $A_t.M_t$.

Although deviations in v_a and v_m can be used to locate inaccurate orientations, the precise level of error is generally difficult to estimate. However, for small errors, e.g., due to sensor noise, the orientation error can be predicted directly from v_a and v_m. Assume that the sensor noise is independent but identically Gaussian distributed in each sensor axis with variance σ_a^2 and σ_m^2 in the accelerometer and magnetometer signals, respectively. With low noise levels, i.e., $\sigma_a < 0.1$ g and $\sigma_m < 0.1$ b,

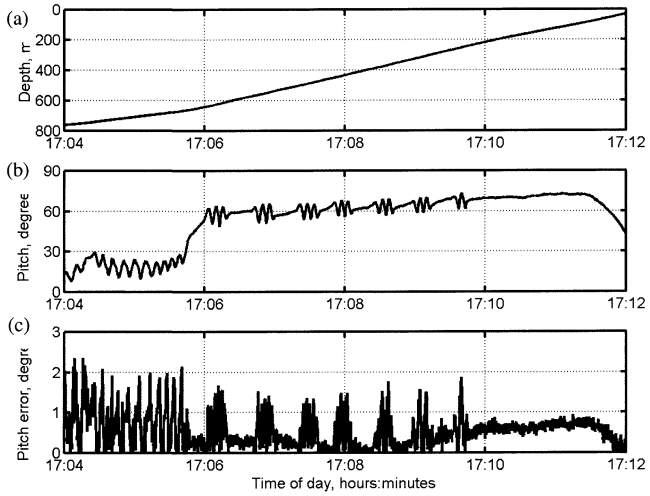

Fig. 5. Sperm whale ascent example showing (a) depth; (b) whale frame pitch; and (c) pitch error estimate.

the standard deviations of v_a, v_m, p, r, and h can be estimated using a Monte Carlo method as

$$\mathrm{std}(v_a) \approx \sigma_a \quad \mathrm{std}(v_m) \approx \sigma_m \quad \mathrm{std}(p) \approx \sigma_a$$
$$\mathrm{std}(r) \approx \frac{\sigma_a}{|\cos p|} \quad \mathrm{std}(h) \approx \left(\sigma_a^2 + \frac{\sigma_a^2}{\cos^2 p} + \frac{\sigma_m^2}{b^2 \cos^2 i}\right)^{1/2}. \tag{6}$$

Thus, the pitch accuracy is independent of orientation, while the roll error is increased at high pitch angles due to the $\cos(p)$ scaling factor in (3). Due to the gimballing operation, heading accuracy is dependent on the pitch and roll accuracy as well as the magnetic-field inclination angle. When the inclination angle is large, as it is in high latitudes, the horizontal components of the magnetic field become small, reducing the accuracy of h. The key result in (6) is that $\mathrm{std}(v_a)$ and $\mathrm{std}(v_m)$, which can be measured directly from the tag data, can be used to estimate the sensor noises, σ_a and σ_m, and therefore, the accuracy of the orientation estimate.

In addition to their diagnostic function, v_a and v_m can be used to identify and reduce certain errors in the sensors after a deployment. Miscalibration of the sensors, for example, due to drift or uncompensated pressure and temperature effects, will lead to consistent errors in the orientation estimate correlated with orientation. Provided that the orientation varies widely and often throughout the time series (i.e., is persistently exciting [17]), a locally-linearized least squares method can be used to determine the amount of offset, pressure signal or temperature signal to add to each sensor output so as to minimize the variance of v_a and v_m. For the tag recordings described in the following section, the standard deviations of v_a and v_m were improved from about 0.1 to 0.02 g and from 0.5 to 0.1 μT, respectively, using least squares fitting.

IV. Example Results

The DTAG has been deployed in more than ten field experiments, four involving the northern right whale, *Eubalaena glacialis*, and five focusing on sperm whales, *Physeter macrocephalus*. The right whale deployments took place in the Bay of

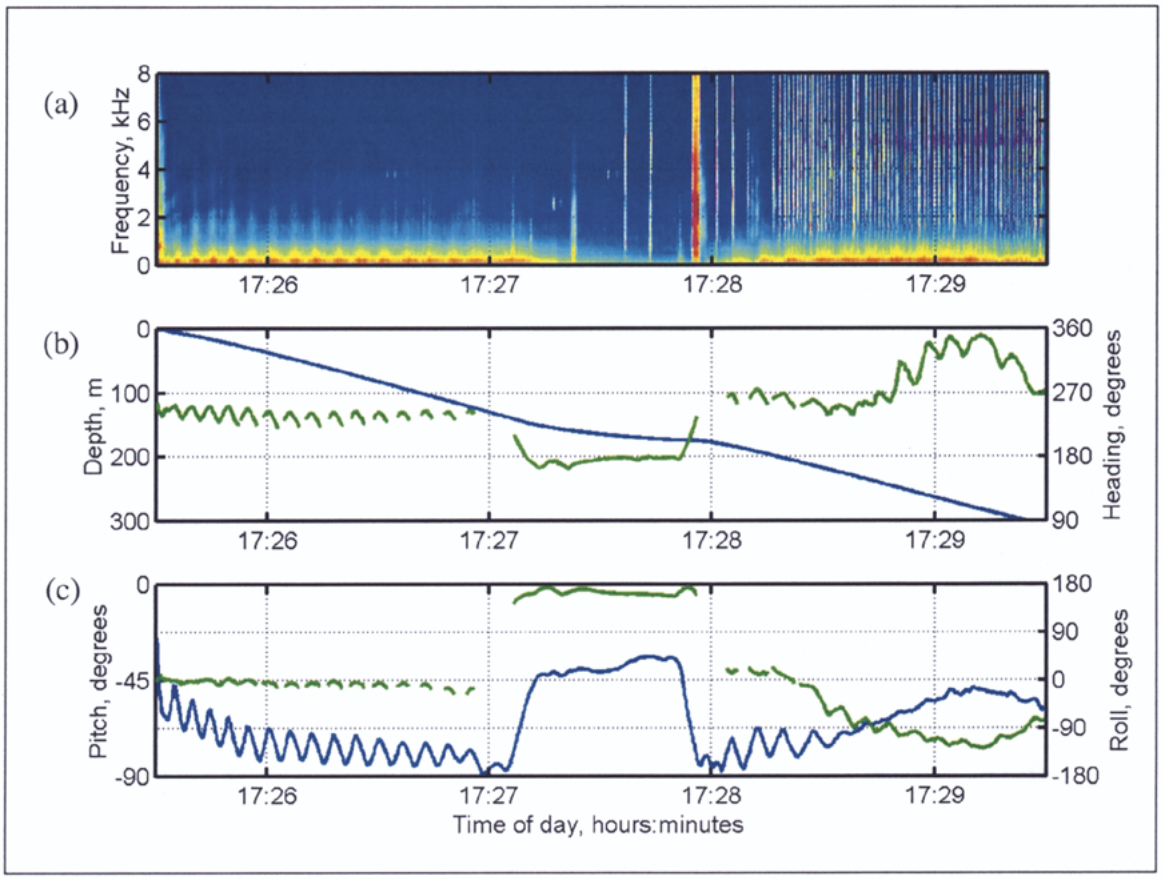

Fig. 6. Interrupted descent of a sperm whale during a sonar playback. The spectrogram of the tag recording (a) shows low-frequency fluke noise and a sequence of clicks from the tagged whale. The dive depth (blue) and heading (green) over the same interval are shown in (b). Pitch (blue) and roll (green) are in (c).

Fundy, in August of each year from 1999 to 2002. The results reported here come from the 2000 field season in which an 8-m launch, operated by Moore for measuring the thickness of the blubber layer on right whales [14], was used to deliver the tags and the 13-m sailing vessel "Song of the Whale," owned and crewed by the International Fund for Animal Welfare, was the observation vessel. An additional small boat was used to deploy a playback sound source.

Sperm whales have been tagged in two areas: the eastern Gulf of Mexico from the R/V Gordon Gunter on National Marine Fisheries Service and Minerals Management Service cruises, and in the Ligurian Sea, between Genoa and Corsica, aboard the R/V Alliance. The Alliance cruises were part of the SIRENA project of the NATO SACLANT Undersea Research Centre [18]. In both areas, the tag was delivered from a small workboat lowered from the ship. The ship itself provided a high platform for visual observations and radio tracking.

Three examples are presented here, selected to show both the range of information that can be inferred from the tag data and to demonstrate the process of establishing a response to a disturbance. The first example illustrates how the tag sensor data can be used to deduce aspects of diving energetics. The second and third examples are potential playback responses elicited from a sperm whale and a right whale, respectively.

Example 1: Sperm Whale Ascent From Depth: The first example is from a SIRENA 2000 deployment on a solo sperm whale. The whale was tagged at 15:23 local time following observation of two dive cycles of about 50 min duration each. Tagging elicited a brief shallow dive but this was followed by long dives consistent with those prior to tagging. The tag recorded for 4.5 h of the 9-h attachment capturing three dives to depths of between 700–960 m and with durations between 40–49 min. Tag data from the ascent portion of the second dive are shown in Fig. 5. The panels in this figure show, from top to bottom, the depth, pitch, and estimated pitch error, all as a function of time. The full ascent took 10 min and the peak vertical velocity was 2 $m \cdot s^{-1}$. Due to the high sensor sampling rate of 23 Hz, individual fluke strokes are revealed in the pitch record. In the initial stage of the Fig. 5 ascent, the animal stroked continuously at a low pitch angle, suggesting travelling. The fluke stroke period was 8 s with a 1.3-s standard deviation. During the final 6 min of the ascent, a high pitch angle was adopted with burst-and-glide swimming. This style of swimming may be an effort to conserve energy [20]. The fluke stroke period in the active swimming bursts is about 6 s and the bursts and intervening glides are of about equal duration until the whale reaches a depth of 200 m. From this point on, ascent is by glide only, presumably powered by the increasing buoyancy of the expanding lungs, an observation found also with northern right whales [21]. The third panel in Fig. 5 gives an estimate for the pitch error using the approximations of (6). The error is small ($<2^\circ$) except during surfacing, indicating that the effects of acceleration, noise, and miscalibration are negligible and that the pitch estimate during ascent is reliable.

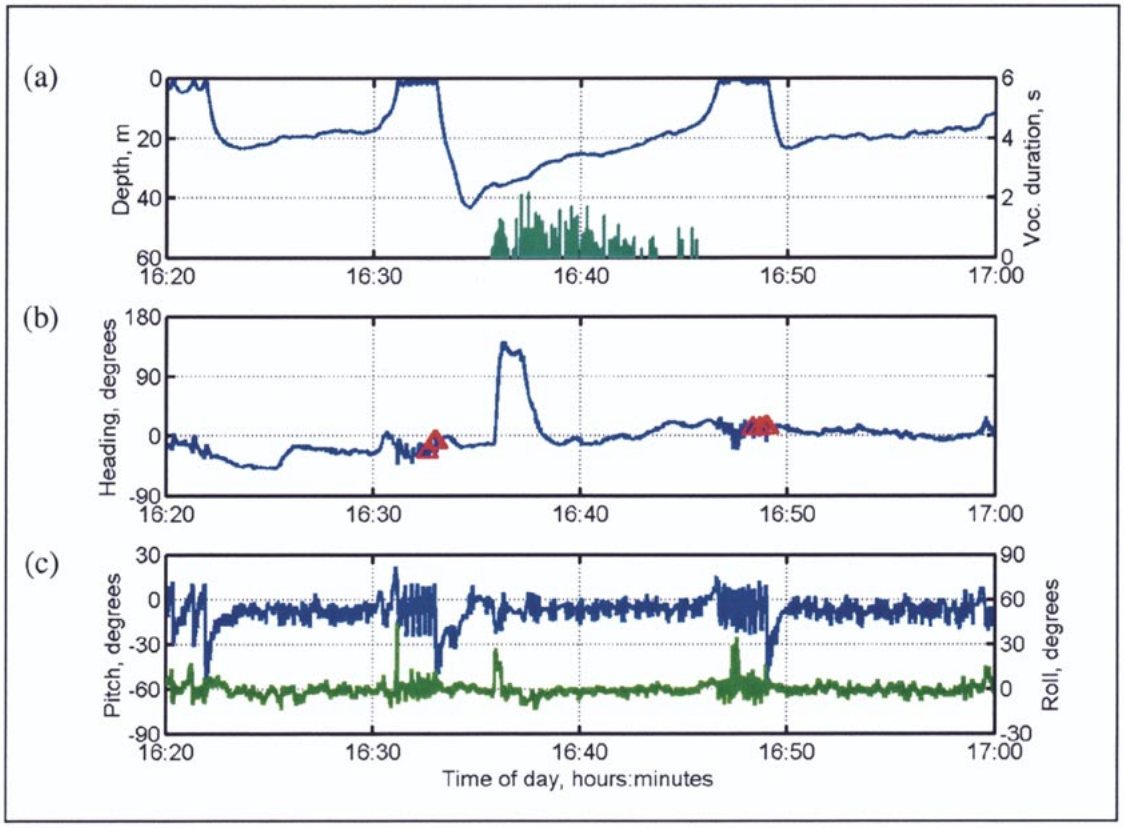

Fig. 7. Right whale response to playback of whale sounds: (a) dive depth; (b) heading; and (c) pitch (blue) and roll (green). The times at which a playback vocalization is audible in the tag recording are shown in (a) as vertical bars with bar height equal to the duration of each vocalization (right-hand axis). Whale headings estimated by visual observers are shown by red triangles in (b).

The reduced energy state suggested by gliding during ascent is indirectly supported by the tag audio record. During the entire period of Fig. 5, the animal was quiet as it was on all long ascents. The primary acoustic component recorded by the tag during ascents is flow noise. In comparison, the whale clicked through 75% of each descent and continuously when at depth.

Example 2: Sperm Whale Descent During Playback: During the deployment described in Example 1, a playback was attempted using a SACLANT-designed sonar deployed from the R/V Alliance [19]. The sonar transducer was towed at a depth of 50 m and produced 50-m·s chirps at 15-s intervals. The center frequency of the chirps was stepped through the series 1, 2.5, 4, and 8 kHz. The source level was approximately 164 dB re 1 μPa at 1 m. The playback started during the second dive, 61 min after tagging, and continued through the third dive. The sonar chirp can be heard clearly on the tag recording as can its echoes from the sea surface and bottom. The received level on the tag varies with depth of the animal due to refraction from the strong thermocline at 50–70-m depth. Despite initiation of the sonar during the second dive, the profile of this dive was similar to that of the first dive. However, the third descent shows a marked departure from the previous two. The three panels in Fig. 6 summarize the audio, depth, heading, pitch and roll during the initial 4 min of the third descent. The upper panel is a spectrogram of the tag recording over a frequency range of 0–8 kHz (the tag sampling-rate was 16 kHz), with local time in hours and minutes as the abscissa. Notable features in this figure, common to the other descents, are flow noise below 1 kHz correlated with fluke-beats, and persistent clicking by the tagged whale starting at a depth of 200 m. The section between 17:27 and 17:28 represents a departure from previous behavior: the fluke noise stops and two intense isolated clicks are followed by a rapid sequence of 8 loud trumpet-like up-sweeps from the host. Also visible in the spectrogram are two huffing sounds, one preceding the clicks and the other immediately following the trumpet sounds. Barely visible in the spectrogram, due to the broad time scale, are the sonar chirps. Both the 2.5- and 4-kHz chirps are seen most clearly after 17:27 when the received level increases.

The remaining panels in Fig. 6 show the depth and orientation of the tagged whale over the same time interval. The lower panel contains the pitch and roll data with the pitch scale on the left-hand side. The dive starts with continuous fluke strokes at a high pitch angle. Beginning at 17:27, there is a pause in swimming and the whale levels to a pitch of $-40\,^{\circ}$. Simultaneously, the animal rolls completely upside-down. About 1 min later, the whale returns to a roll of 0° and resumes swimming. The center panel shows the depth and heading, with the depth ordinate on the left-hand-side. Initially, the vertical velocity (i.e., the slope of the depth-time graph) peaks at 1.6 m·s^{-1} but in the minute following 17:27 the dive levels out due to the reduced pitch angle and pause in swimming. After 17:28, diving recommences at 1.6 m·s^{-1}. A heading change of $80\,^{\circ}$ toward the south also occurs at 17:27, with the animal later returning to its original heading. The gaps in the roll and heading plots indicate where the error estimates of (6) exceed $10\,^{\circ}$ or where

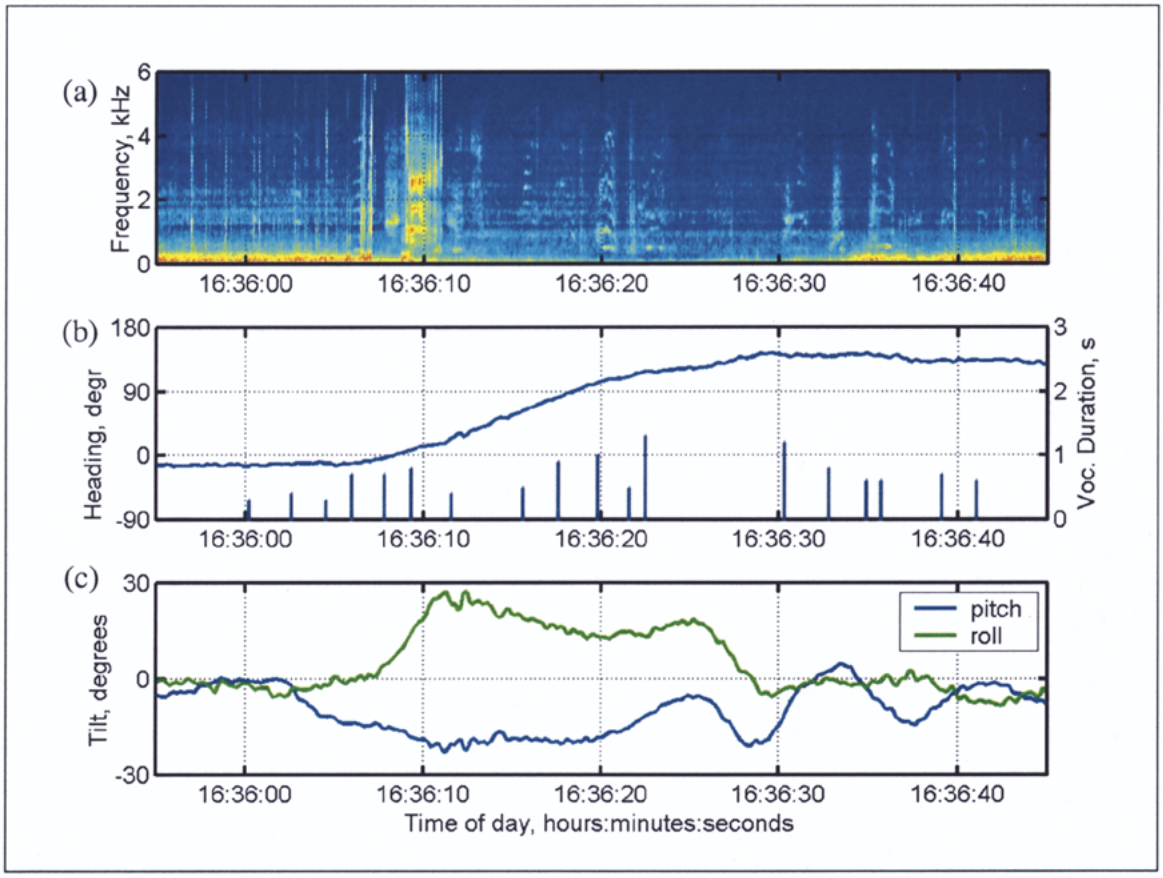

Fig. 8. Close up of the right whale response to playback of whale sounds. (a) The spectrogram of the tag recording shows a number of faint vocalizations (from the playback) and a reduction in flow and/or fluke noise. Bars on (b) show the times at which playback vocalizations are audible (duration is on the right-hand axis). Pitch (blue) and roll (green) are shown in (c).

the pitch exceeds 80°, resulting in unreliable orientations. The pitch error is $<2°$ throughout the example.

The maneuver starting at 17:27 combines three movements: i) a pitch decrease from $-80°$ to $-40°$; ii) a roll upside-down; and iii) a heading change of 80° southward. Given the orientation ambiguity described in Section III, an equivalent explanation for the maneuver is: i) a pitch change from $-80°$ to $-140°$, and ii) a heading change from 250° to 330°, with roll remaining at 0°, i.e., the animal pitches almost upside-down and turns to the south (note that, when the animal is pitched past 90°, a 360° heading is due south). At this time, both the R/V Alliance and the workboat were roughly due south-east of the animal at ranges of about 2 km and 600 m, respectively. Although not apparent in the audio record from the tag, the workboat increased speed at about the same time as the maneuver of Fig. 6. The question is, does this maneuver represent a response to the sonar or the workboat or neither? The turn toward the south is coincident with an increase in received level of the sonar. However, by 17:27, the sonar had been broadcasting for 1 h already, eliminating the possibility of surprise. Likewise, the workboat had recently been much closer to the animal. Clearly, more baseline data and carefully conducted sound exposures are required before a conclusion can be made as to which stimulus elicited the response.

Example 3: Right Whale Response to a Playback: A less ambiguous response to playback was elicited from a northern right whale in August 2000. The animal was tagged at 13:30 local time and reacted to tagging with a short shallow dive. The tag remained attached for 3.7 h until it was knocked off in a social group. In this time, the tagged whale performed nine dives below 100 m, with the deepest being 207 m, and an additional ten shallower dives to about 40 m. The dives were short and the whale's behavior was classified as travelling. Two 10-min duration playbacks were made to the tagged animal using a J-11 underwater sound source. The first, starting 110 min after tagging, consisted of vessel sound recorded previously from a passing tanker. The tanker speed was about 15 kn, and the playback amplitude was tapered so as to start and end gradually. The source level was approximately 170 dB re 1 μPa at 1 m, and the range to the tagged whale was 600 m. No response was found in the tag data to this playback. The second playback started 186 min after tagging, and comprised a recording from a group of right whales previously socializing in the same area. The playback contained about 100 tonal and pulsatile sounds [3, ch. 7] and 12 noisy blows.

The response to the whale sound playback is shown in Fig. 7. The panels in this figure are depth (top), heading (center), and pitch and roll (lower), for three dives bracketing the playback. The time and duration of each vocalization in the playback are indicated by the vertical bars in the top panel, where the scale on the right-hand side is duration in seconds. No other vocal activity was recorded during the 40 min displayed here. Red triangles on Fig. 7(b) indicate visual observations of the surfacing whale made at ranges between 400–600 m with a calibrated video camera. The observed heading is very close to the tag

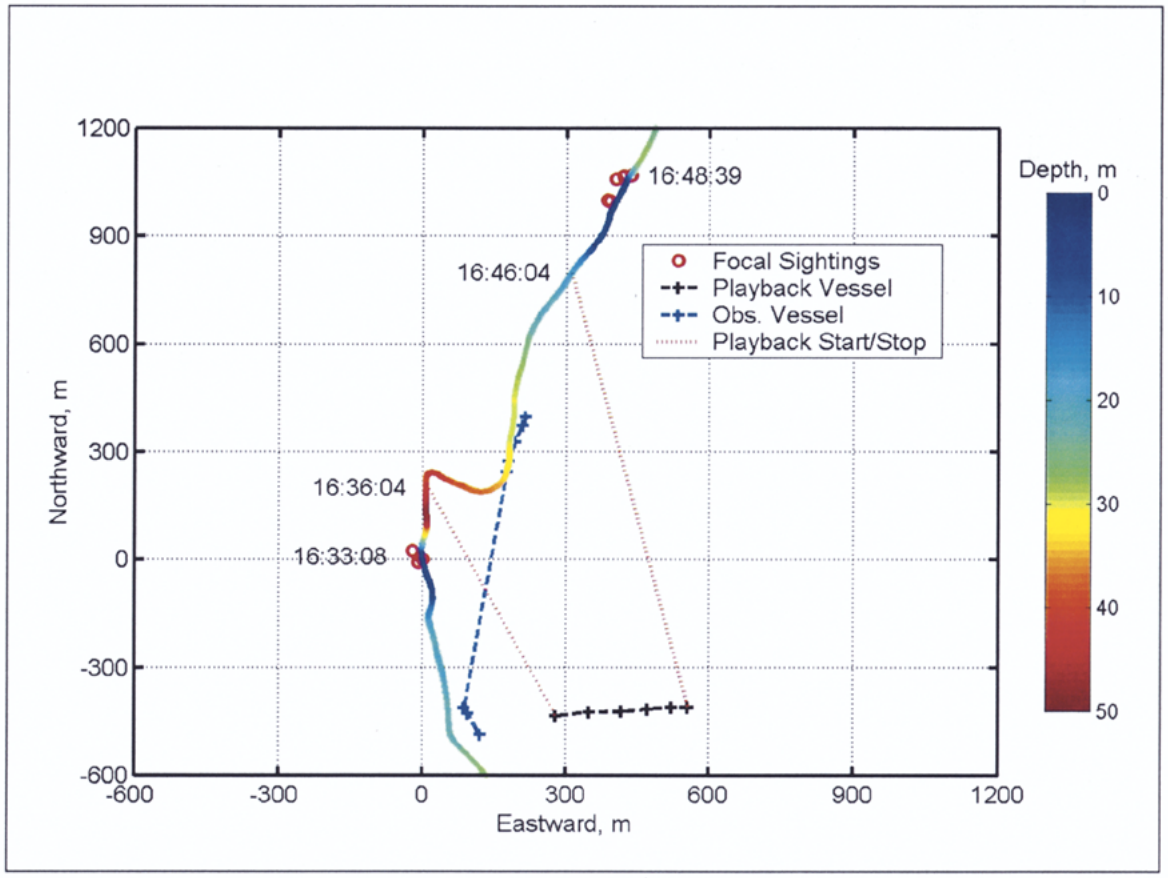

Fig. 9. Tracks of the tagged right whale and participating vessels during the playback of whale sounds. The dead-reckoned track of the whale is shown as the colored line, with color indicating depth. The red dashed lines show the positions of the whale and the playback vessel at the start and end of playback. The east and north scales are in meters with the zero point placed at the surfacing position preceding the playback.

heading, confirming the reliability of the tag data. A significant heading change (150 °) is evident in Fig. 7(b) at the start of the playback. This transient is unique in the tag record. The whale held the new heading for 65 s and then gradually returned to its original heading. In contrast with the sperm whale example, the pitch and roll records show little activity except for a banking roll of 20 ° accompanying the heading change. Orientation errors, estimated using (6), are less than 3 ° over the time shown.

In order to establish the relative timing of the playback and heading change, a 50-s excerpt from Fig. 7 is shown in Fig. 8. In this figure, the top panel is a spectrogram of the tag audio recording with a frequency range of 0–6 kHz. The tonal playback sounds are the short duration harmonic structures (e.g., at 16:36:20). Fluke noise, present at the beginning of the excerpt, disappears during the turn and starts again at the new heading. The center panel in Fig. 8 shows heading and the vertical bars indicate where playback sounds were recorded by the tag. The heading change begins about 7 s after the start of the playback. The lower panel contains the pitch and roll, both over a −30 °–30 ° range. The small changes in pitch and roll also follow the start of the playback.

Fig. 9 shows the relative positions of the right whale, playback vessel, and observation vessel during the playback. The track of the right whale (the line colored by depth in Fig. 9) was produced by dead-reckoning based on the tag heading and pitch data. To do this, the speed-over-ground of the whale was estimated from

$$\begin{bmatrix} v_e \\ v_n \end{bmatrix} = s_w \cos(p) \begin{bmatrix} \sin(h) \\ \cos(h) \end{bmatrix} + s_c \begin{bmatrix} \sin(\phi) \\ \cos(\phi) \end{bmatrix} \tag{7}$$

where v_e and v_n are the eastward and northward velocity components of the whale; s_w and s_c are the whale's speed-through-water and the water current, respectively; h is the whale's heading from the tag (in degrees true); ϕ is the heading of the water current. The $\cos(p)$ term in (7) corrects for vertical motion of the whale. Both s_c and s_w are assumed to be constant, s_c and ϕ were initially estimated from the drift of the playback vessel (0.5 m·s^{-1}, due east). Then, s_c and s_w were adjusted to fit the dead-reckoned track to the surface observations. The final values chosen were 0.3 m·s^{-1} for s_c and 1.3 m·s^{-1} for s_w. Finally, the track in Fig. 9 was obtained by integrating (7).

The key point in Fig. 9 is that, immediately after the start of playback, the whale turned toward the playback vessel. Combining this with the causality illustrated in Fig. 8, we conclude that the whale responded to the playback. The distance between playback vessel and whale was 700 m at the start of playback and the received level was roughly 115 dB re 1 μPa. After about 1 min, the whale resumed its preplayback course. In assessing the significance of the response shown in Fig. 9, there are some

important caveats. The first is that the constant whale speed used in dead-reckoning does not take into account the absence of fluke strokes during the initial response period, evident in Fig. 8(a). As a result, travel toward the playback vessel is probably exaggerated in Fig. 9. Secondly, the presence of the observation vessel (the blue dashed line in Fig. 9), a yacht under motor propulsion, between the playback source and the whale presents a confound. Field work is continuing to establish baseline behavior and to perform a statistically significant set of playbacks. Nonetheless, this example demonstrates the ability of the tag to capture subtle, short-term subsurface responses.

V. Conclusion

The DTAG has been designed specifically for studies on how wild marine mammals respond to sound. The noninvasive tag provides short-term but highly detailed information about the acoustic environment and behavior of the host animal. By combining accelerometer and magnetometer signals, the orientation of the animal can be determined accurately and with sufficient resolution to capture individual fluke-strokes and subtle movements. Results from tagging two large whale species demonstrate the broad range of inferences that can be made from the tag data and suggest that it can detect most movements and vocal behaviors of a whale continuously throughout the dive cycle. In addition to establishing behavioral responses to natural and anthropogenic sounds, it may be possible to use tag data to estimate the energetic cost of such responses. This information is sorely needed in setting suitable exposure levels for sound from commercial, defense and research activities and in establishing effective mitigation protocols.

Acknowledgment

The authors gratefully acknowledge the contributions of: A. Shorter, P. Miller, T. Hurst, J. Partan, M. Moore, N. Biassoni, S. Parks, C. Carlson and C. Miller of WHOI; D. Nowacek of NMFS Northeast; A. Bocconcelli of UNCW; B. Gisiner of ONR; B. Lang of MMS; D. Allen of the Smithsonian Institution; W. Hoggard, T. Martinez and K. Mullin of NMFS Southeast; F. Deckert and F. Townsend of Tracpac; W. Zimmer, A. D'Amico and M. Carron at SACLANTCEN; S. Kraus of the New England Aquarium; crews of the R/Vs Song of the Whale, G. Gunter, and Alliance. In memory of Emily Argo.

References

[1] R. J. Urick, *Ambient Noise in the Sea*. Los Altos, CA: Peninsula, 1986.
[2] D. M. Green, H. A. DeFerrari, D. McFadden, J. S. Pearse, A. N. Popper, W. J. Richardson, S. H. Ridgway, and P. L. Tyack, "Low-frequency sound and marine mammals: Current knowledge and research needs," National Academy Press, Washington, DC, NRC Rep., 1994.
[3] W. J. Richardson, C. R. Greene, Jr., C. I. Malme, and D. H. Thomson, *Marine Mammals and Noise*. New York: Academic, 1995.
[4] A. Frantzis, "Does acoustic testing strand whales?," *Nature*, vol. 392, no. 29, p. 29, 1998.
[5] P. J. O. Miller, N. Biassoni, A. Samuels, and P. L. Tyack, "Whale songs lengthen in response to sonar," *Nature*, vol. 405, p. 903, 2000.
[6] K. J. Finley, G. W. Miller, R. A. Davis, and C. R. Greene, "Reactions of belugas, *Delphinapterus leucas*, and narwhals, *Monodon monoceros*, to ice-breaking ships in the Canadian High Arctic," *Can. Bull. Fish. Aquat. Sci.*, vol. 224, pp. 97–117, 1990.
[7] S. E. Cosens and L. P. Dueck, "Responses of migrating narwhal and beluga to icebreaker traffic at the Admiralty Inlet ice edge, N.W.T. in 1986," in *Proc. Conf. Port Ocean Engineering Under Arctic Conditions*, W. Sackinger, Ed., Fairbanks, AK, 1998, pp. 39–54.
[8] W. A. Watkins and W. E. Schevill, "Sperm whales (*Physeter catodon*) react to pingers," *Deep-Sea Res.*, vol. 22, pp. 123–129, 1975.
[9] W. C. Burgess, P. L. Tyack, B. J. LeBoeuf, and D. P. Costa, "A programmable acoustic recording tag and first results from free-ranging northern elephant seals," *Deep-Sea Res.*, vol. 45, pp. 1327–1351, 1998.
[10] S. Fletcher, B. J. Le Boeuf, D. P. Costa, P. L. Tyack, and S. B. Blackwell, "Onboard acoustic recording from diving northern elephant seals," *J. Acoust. Soc. Amer.*, vol. 100, pp. 2531–2539, 1996.
[11] D. Nowacek, P. L. Tyack, R. Wells, and M. Johnson, "An onboard acoustic data logger to record biosonar of free-ranging bottlenose dolphins," *J. Acoust. Soc. Amer.*, pt. 2, vol. 103, no. 5, p. 2908, 1999.
[12] V. Papastavrou, S. C. Smith, and H. Whitehead, "Diving behavior of the sperm whale, *Physeter macrocephalus*, off the Galápagos Islands," *Can. J. Zool.*, vol. 67, pp. 839–846, 1989.
[13] R. W. Baird, "Studying diving behavior of whales and dolphins using suction-cup attached tags," *Whalewatcher*, vol. 32, no. 1, pp. 3–7, 1998.
[14] M. J. Moore, C. A. Miller, M. S. Morss, R. Arthur, W. Lange, K. G. Prada, M. K. Marx, and E. A. Frey, "Ultrasonic measurement of blubber thickness in right whales," *J. Cetacean Res. Management*, vol. 2, pp. 301–309, 2001.
[15] W. T. Thompson, *Introduction to Space Dynamics*. New York: Dover, 1986.
[16] F. E. Fish, J. E. Peacock, and J. Rohr, "Phase relationships between body components of odontocete cetaceans in relations to stability and propulsive mechanisms," in *Proc. 1st Int. Symp. Aqua Bio-Mechanisms*, Aug. 2000, pp. 57–60.
[17] L. Ljung, *System Identification: Theory for the User*. Englewood Cliffs, NJ: Prentice-Hall, 1999.
[18] W. M. X. Zimmer, M. Johnson, A. D'Amico, and P. Tyack, "Combining data from a multisensor tag and passive sonar to determine the diving behavior of a sperm whale (*Physeter macrocephalus*)," *J. Oceanic Eng.*, vol. 28, pp. 13–28, Jan. 2003.
[19] J. E. Bondaryk and A. D'Amico, "Low-power active Sonar for marine mammal risk mitigation," *J. Oceanic Eng.*, to be published.
[20] D. A. Pabst, "Morphology of the subdermal connective tissue sheath of dolphins: A new fiber-wound thin-walled, pressurized cylinder model for swimming vertebrates," *J. Zool.*, vol. 238, pp. 35–52, 1996.
[21] D. Nowacek, M. Johnson, P. Tyack, K. Shorter, W. McLellan, and D. Pabst, "Buoyant Balaenids: The ups and downs of buoyancy in right whales," *Proc. R. Soc.B.*, vol. 268, pp. 1811–1816, 2001.

Mark P. Johnson was born in England in 1966. He received the B.E. and Ph.D degrees in electronic engineering from the University of Auckland, Auckland, New Zealand, in 1986, and 1992, respectively.

Following post-graduate work with the Acoustic Research Center, Auckland University, Auckland, New Zealand, he joined the Woods Hole Oceanographic Institution, Woods Hole, MA, in 1993, where he is currently a Research Engineer in the Department of Ocean Physics and Engineering. He is interested in engineering approaches to studying marine mammals and in developing miniature electronic systems for underwater sensing.

Dr. Johnson is a Member of the Acoustical Societies of America and New Zealand.

Peter L. Tyack was born in Boston, MA, on December 31, 1953. He received the A.B. degree in biology (*summa cum laude*) from Harvard College, and the Ph.D. degree in animal behavior from Rockefeller University, in 1976, and 1982, respectively.

He joined the the Woods Hole Oceanographic Institution, Woods Hole, MA, as a Postdoctoral Scholar, in 1982, and is currently a Senior Scientist and Walter A. and Hope Noyes Smith Chair in the Biology Department. He is interested in social behavior and acoustic communication in whales and dolphins and has conducted research on bottlenose dolphins, sperm whales, humpback whales, gray whales, right whales, and bowhead whales. He has focused on developing new techniques to monitor vocal and social behavior of marine mammals, including methods to tag whales, locate their calls, and for video monitoring of behavior.

Dr. Tyack is a charter member of the Society for Marine Mammalogy and Fellow of the Acoustical Society of America.